Mass Spectrometry

Continuous Two-Channel Time-of-Flight Mass Spectrometric Detection of Electrosprayed Ions**

*Oliver Trapp, Joel R. Kimmel, Oh Kyu Yoon, Ignacio A. Zuleta, Facundo M. Fernandez, and Richard N. Zare**

Time-of-flight mass spectrometry (TOFMS) is a widely used technique that is recognized for offering high analytical performance at a reasonable cost. Development of this technique is ongoing, and advances in areas such as ion optics and ion-detection hardware have pushed the mass resolution and mass accuracy of TOFMS to regimes that are appropriate for the identification of components of complex mixtures.[1] The technique's intrinsic high ion transmission and capability to measure wide mass ranges without scanning, yields high sensitivity and fast spectral acquisition rates. Based on these characteristics, TOFMS seems to be an ideal detector for fast separations of analytes with a broad range of molecular weights.[2] Such applications, which include the in-line separation of pharmaceuticals, peptides, or proteins followed by electrospray ionization, are becoming increasingly important.[3] Unfortunately, the pulsed nature of TOFMS yields inherent losses when analyzing ions emerging from continuous ion sources. Minimization of these losses can be achieved only at the expense of a reduction in the sampled mass range and potentially the mass resolution if the flight path is shortened. In conventional TOFMS, packets of ions are periodically pulsed into the entrance of a field-free drift chamber. To avoid overlap of the recorded flight times, the duration between start pulses is set to be longer than the flight time of the heaviest analyte ion. Ions reaching the entrance of the flight chamber between start pulses are lost. Thus, the ion sampling efficiency (duty cycle) and spectral acquisition speed are directly related to the ratio of the duration of the start pulse to the time between pulses, and these figures of merit decrease as the sampled mass range or flight path are increased.

[*] Dr. O. Trapp, J. R. Kimmel, O. K. Yoon, I. A. Zuleta, Prof. Dr. F. M. Fernandez,[+] Prof. Dr. R. N. Zare
Department of Chemistry
Stanford University
Stanford CA 94305-5080 (USA)
Fax: (+1) 650-723-9262
E-mail: zare@stanford.edu

[+] Present address:
School of Chemistry and Biochemistry
Georgia Institute of Technology
Atlanta, GA 30332-0400 (USA)

[**] This work was supported by the US Air Force Office of Scientific Research (AFOSR Grant FA9550-04-1-0076) and Predicant Biosciences, South San Francisco. O.T. thanks the Deutsche Forschungsgemeinschaft (DFG) for an Emmy Noether-Fellowship (TR542/1-1/2) and F.M.F. thanks the Fundacion Antorchas for a postdoctoral fellowship. J.R.K. was supported by an American Chemical Society Division of Analytical Chemistry Fellowship, sponsored by Merck & Co.

An ideal detector for capillary and chip-format separations should provide universal detection, sufficient spectral selectivity, and high sensitivity without degrading separation efficiency.[4] If TOFMS is to become the detector of choice for these applications, optimization of its transmission, speed, and efficiency is essential. One approach to improve the duty cycle is to modulate the continuous ion beam of a conventional TOF instrument to receive encoded single-ion packets, for example, by Fourier transform techniques.[5] The mass spectrum is then obtained by mathematical deconvolution and the analyzer duty cycle can be increased to about 25%.

The most widely used strategy for improving the duty cycle of TOFMS is orthogonal extraction (OE).[6] In this TOFMS configuration the fraction of the ion beam that is sampled is proportional to the length of the extraction region in the dimension orthogonal to the field-free flight trajectory. This region tends to be much larger than the sampling volume defined by ion gates used in an on-axis configuration. Thus, OE-TOFMS has a higher duty cycle than conventional on-axis TOFMS. But, because the flight times of ions traversing the extraction region depend on m/z, the duty cycle of OE-TOFMS decreases with m/z. More importantly, the overall performance of OE-TOFMS is still limited by trade-offs between efficiency, mass resolution, and mass range.

In an effort to decouple these figures of merit, we continue to explore a TOFMS strategy based on Hadamard-type, pseudorandom modulation.[7] In this case a finely spaced Bradbury–Nielson gate (BNG)[8] is used to rapidly modulate (MHz frequency range) a continuous ion beam on and off the axis of detection following a known pseudorandom binary sequence. Encoding sequences are applied to the ion beam by alternating the voltage of this gate between two set limits; a sequence element "1" fixes the gate electrodes at relative ground and allows ions to pass undeflected, while a sequence element "0" shifts the gate electrodes to a deflecting state. The acquired spectrum corresponds to the sum of time-shifted spectra of multiple packets. Knowledge of the encoding sequence allows mathematical deconvolution and recovery of the TOF mass spectrum. The length of the applied encoding sequence is chosen based on the range of flight times (i.e. mass range) being monitored. All encoding sequences contain approximately equal numbers of 1s and 0s (on and off signals), so by detecting all ions of state "1", a one-channel Hadamard transform (HT) TOF mass spectrometer offers a 50% duty cycle, independent of other instrument parameters.

In an attempt to extend the duty cycle of HT-TOFMS to 100% and to increase the overall performance of the technique, for example, the signal-to-noise ratio (SNR), a next generation instrument has been developed as shown in Figure 1a. Improvements include new modulation electronics[9] which integrate the Bradbury–Nielson gate on the driver board to minimize the length of the transmission lines for the amplified modulation sequence for more precise and also faster modulation, and software for simultaneous data acquisition and real-time Hadamard transformation. New focusing optics allow us to obtain a highly focused ion beam with a narrow energy distribution that can be precisely deflected at the BNG with a switching frequency between 5 and 50 MHz corresponding to an encoding element width of

 DOI: 10.1002/anie.200461240

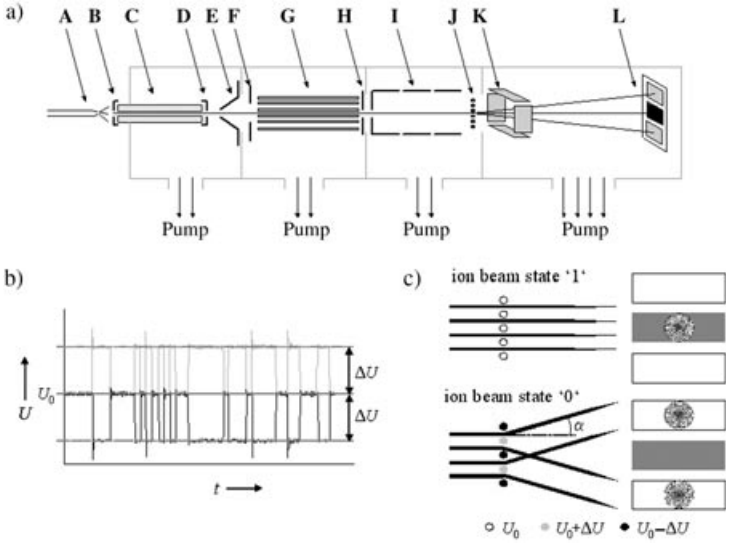

Figure 1. a) Schematic experimental setup of the new HT-TOF mass spectrometer. A) Electrospray needle, B) counter electrode, C) heated glass capillary, D) capillary exit electrode, E) skimmer, F) focusing lens, G) hexapole, H) conductance limiting exit lens, I) Einzel lens, J) Bradbury–Nielson gate, K) *x*,*y* steering plates, and L) masked dual-anode detector. b) Oscilloscope traces of the positive and negative phases of a Hadamard modulation sequence segment (1111110000111111010101011000001000010000011001100) applied to the Bradbury–Nielson gate. c) Dual-detection scheme demonstrating the ion-beam states "0" and "1".

200 and 20 ns, respectively. The deflection angle α of the modulated ion beam (see Figure 1c) can be controlled by varying the voltage (ΔU) applied to the BNG. With sufficient modulation voltage applied to the BNG two spatially resolved modes of the ion beam can be experimentally observed at the detector plane: a centered, focused beam, and the two deflected ion beam branches that arrive above and below the detector center. To monitor both spatial modes, we have designed and installed a dual-anode multichannel plate (MCP) detector with isolated active charge-collection areas and a mask that is dimensioned to reflect the spatial profile of the modulated ion beam (Figure 1c).

The maximum duty cycle of a one-channel HT-TOF mass spectrometer is 50%. The experimentally achieved value depends on the percentage of ions entering the mass analyzer that strike the detector and, further, on the fraction of these ions that are modulated on and off of the detector [Eq. (1)] where n_{tot} is the total number of ions entering the mass analyzer, n_t is the number of ions striking the detector in the transmitted mode, and n_{nt} is the number of ions striking the detector (ideally zero) in the non-transmitted mode.

$$\text{duty cycle} = 50\,\% \left(\frac{n_t}{n_{tot}}\right)\left(\frac{n_t - n_{nt}}{n_t}\right) \qquad (1)$$

The first ratio in Equation (1) represents ion-beam clipping, which can result if the ion beam and the detector are not properly aligned. The second ratio describes the deflection efficiency during modulation of the ion beam. The "0"-state ions that are insufficiently deflected and strike the detector yield no TOF information and contribute to background noise.

Two-channel HT-TOF mass spectrometry involves the simultaneous optimization of paired one-channel HT-TOFMS experiments. Detecting high-quality spectra on the outer channel requires that deflection not only moves ions off the central axis of detection, but also that the deflection is repeatable and well-defined. While the inner channel records the static, focused component of the modulated ion beam, the outer channel detects ions that have undergone a time- and energy-dependent deflection (impulse sweep mode).[10] Optimized conditions for both channels require reducing the kinetic-energy spread of the ions and matching the images of the deflected and undeflected ion-beam modes at the plane of the detector with the detector dimensions.

Images of the deflected and undeflected ion-beam modes were collected for the "0" and "1" modulation states using various optical configurations. The voltages applied to the set of four steering plates (see Figure 1a) at the entrance of the TOF chamber were scanned to move the ion beam about the three active areas of the detector. Synchronized measurements of total ion current (TIC) were used to generate two-dimensional ion-current plots. These plots represent the convolution of the detector shape and the beam shape. In the situation where the beam cross section is small compared to the detector area, the ion-current plot will have the shape of the beam, and knowledge of the detector dimensions can be used to estimate beam size. These data were used to optimize beam focus and position and to choose appropriate modulation conditions. Figure 2 displays the beam images at optimized conditions. The focused ion beam has dimensions comparable to the inner anode and can be moved vertically between the three active areas. The deflected ion beam has two well-defined centers that exist above and below the focused mode (Figure 2c and d).

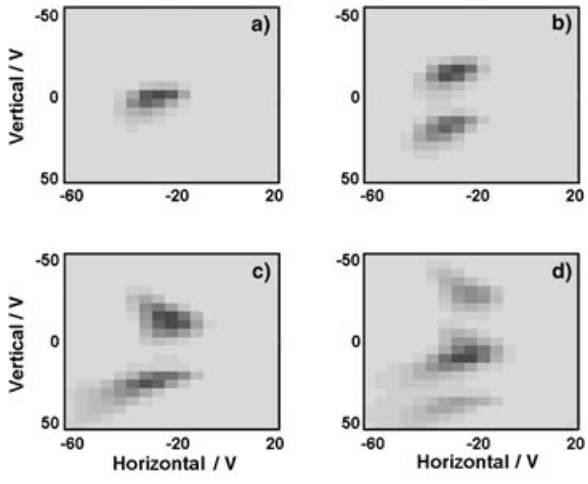

Figure 2. Two-dimensional images of the position, shape, and size of the temporally and spatially modulated ion beam obtained by *x*,*y*-steering of the undeflected or deflected ion beam across the two detection anodes. a) Undeflected ion beam detected at the inner anode, b) undeflected ion beam detected at the outer anode, c) deflected ion beam ($\Delta U = 13$ V) detected at the inner anode, d) deflected ion beam at the outer anode.

Subtracting deflected data from the undeflected data collected under identical scanning conditions provides a measure of how many ions are modulated about each detector at a specific beam position and focus. High duty cycle requires that ion current moves between the two channels of detection. Poor alignment or non-ideal deflection yield asymmetry in the data obtained for the two channels. Figure 3 shows an example of such data extracted from vertical cross sections with a modulation voltage $\Delta U = 13$ V applied to the BNG. The changes in the sign and magnitude of the deflection verify that the deflection process is vertical and that the deflected mode of the ion beam has two branches. At the ideal position, the BNG moves the entire ion beam from the inner to the outer anode.

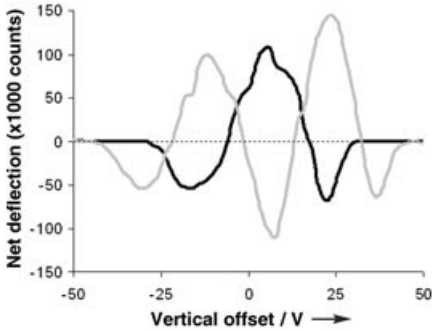

Figure 3. Net deflection plots of reserpine ($C_{33}H_{40}N_2O_9$) extracted by substracting the vertical cross-sections of the deflected mode from the vertical cross sections of the undeflected mode of the ion beam. The black and gray curves represent the inner and outer detection anodes, respectively.

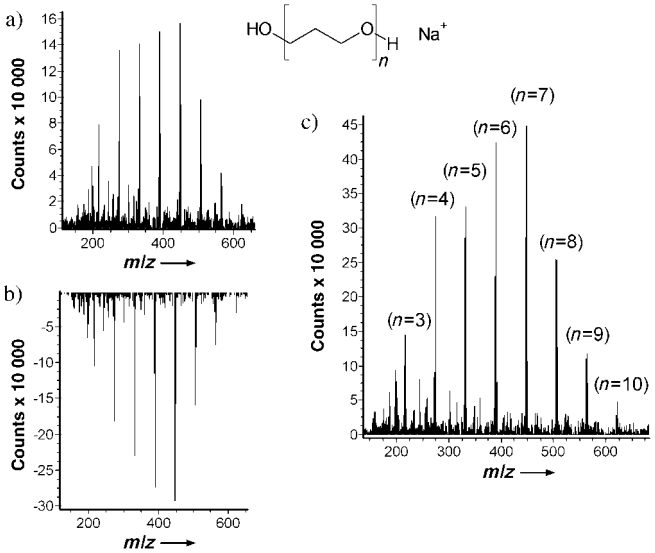

Figure 4. Spectra of PPG 450 simultaneously collected at the inner (a) and outer (b) anodes of the detector. Spectrum (c) represents the difference of spectrum (a) and spectrum (b) with an experimental improvement of the SNR of 29%. Conditions are 11-bit modulation sequence (2047 elements), 20 MHz modulation frequency, and 30 s acquisition time.

Figure 4 shows deconvoluted spectra of polypropylene glycol (PPG 450) acquired at the inner and outer anodes. The spectrum of the outer anode is inverted owing to the mathematical formalism of the multiplication of the inverse Hadamard matrix (in our experiment a simplex matrix)[11] with the raw spectrum of the outer anode, where each on state of the beam at the inner channel corresponds to the off state of the beam at the outer and vice versa. Similar data were collected for analytes across an m/z range of 200 to 2000 amu, including: caffeine, tetrabutylammonium acetate, *N*-hydroxyethyl-*N*,*N*-dimethylbenzylammonium chloride, bradykinin, reserpine, PPG 1000, and gramicidin. In each case, the flight times measured on the two channels were identical, and data subtraction did not require peak matching of the two spectra. At faster modulation and acquisition rates the slight difference in the flight paths to the two channels could require a different procedure to match and calibrate data.

Under ideal conditions the combination of the two channels of data yields an improvement of 41% ($\sqrt{2}$) in SNR over the one-channel experiment (only the inner detector). Experimentally we observe an average SNR improvement of 29%. Small deviations in the beam-detector proportions primarily cause this difference. Two-channel experiments were also carried out with a two-stage reflectron installed. Resolvable ion beamlets were observed in beam-imaging experiments, but the extension of the flight path (2.2 m) caused a majority of the deflected ions to miss the outer detector at even our lowest deflection voltage ($\Delta U =$ 13 V). Thus, the duty cycle on this detector was limited by the beam clipping term in Equation 1. Using current knowledge of the ion-beam dimensions and deflection profiles, appropriately sized detection areas will be designed to detect all ions.

With the implemented instrumental modifications, this two-channel detection scheme extends the achievable duty cycle of HT-TOFMS to 100% and effectively converts TOFMS into a continuous detection technique. Beyond the improved SNR, this advance gives an increase in the data acquisition rate (several thousand full spectra per second). More generally, this work suggests that temporal and spatial encoding of ion beams combined with multichannel detection schemes is a promising strategy for increasing the information density of TOFMS experiments.

Efficient multiplexing enables novel approaches to tandem MS detection. For example, the three spatially defined regions in this experiment (Figure 2) could be used for different MS experiments. It can be envisioned that one of the beams might be used for high-speed HT-TOFMS while the other two ion beams could be transferred into a high-mass resolution ion-trapping instrument, such as a Fourier transform ion cyclotron resonance mass spectrometer (FT-ICR-MS)[12] for MS^n experiments.

Experimental Section

Figure 1 a illustrates the experimental setup of the ESI-HT-TOF mass spectrometer at Stanford University. Ions are produced by an ESI source consisting of three differentially pumped stages. A borosilicate

glass capillary (0.4 mm i.d., length 124 mm), treated with chlorotrimethylsilane (Fluka) to minimize analyte surface interactions, was used as the transfer line between atmospheric pressure and the first pumping stage. A fused silica capillary, mechanically sharpened and coated with gold was used as spray needle. Analyte solutions were infused into this fused silica capillary at flow rates between 0.1 and 10 μL min^{-1} by application of back pressure. The typical electrospray conditions were: spray-needle voltage of +2.4 to +3.6 kV, needle–capillary separation of 5–8 mm, and a spray source temperature of 220 °C. The metal front and end cap of the heated transfer capillary were set between +30 and +80 V. Ions were extracted from the silent zone of the mach disk emerging from the metal spray nozzle with a skimmer (1 mm orifice i.d., +20 to +50 V). The second pumping stage of the ion source consists of a focusing lens (+14 to +24 V), a hexapole ion guide (length 21.9 cm, frequency 2.9 MHz, amplitude between 200 and 2500 V; ABB Inc, Pittsburgh), and a focusing exit lens (−2 to −25 V). The ions were accelerated to kinetic energies of 1500 eV by the first segment of a modified Einzel-type lens. Angular spread caused by the acceleration is focused by varying the voltage of the middle lens of the Einzel lens (−420 to −500 V). After the Einzel lens, a Bradbury–Nielson gate modulates the ion beam. The modulator grid consists of interspersed wire sets positioned normal to the ion beam. The wire sets were made from 20-μm diameter gold-plated tungsten wire and spaced 100 μm apart.[8b] The pseudorandom sequence generator (Predicant Biosciences) is based on a feedback shift register circuit producing variable length sequences between 255 (8-bit) and 16383 (14-bit) elements. The modulation frequency can be set between 2 and 50 MHz and was kept at 20 MHz for all the experiments reported herein. The low-voltage signals of the binary sequence are transmitted to a driver board which is mounted on a heat sink cooled by a water/Peltier element. The cooling system is rated to dissipate up to 80 W of heat generated during operation. At the driver board the low voltage modulation signal is split into two phases that are 180° out of phase, amplified to voltages between $\Delta U = 13$ and 24 V, and applied to the wire sets of the Bradbury–Nielson gate, which floats at the flight tube potential (−1500 V). The ion beam passes undeflected when both wire sets are at the same potential, corresponding to the beam "on" state (1). When opposing potentials (between $\Delta U = 13$ and 24 V) are applied to the wire sets, the beam is split into two deflected beams, corresponding to the beam "off" state (0). The effective flight path in the non-reflectron configuration corresponds to approximately 1.1 m. The ions, passing through the slits of mask in front of the detector, are post-accelerated to an energy of 2300 eV before they are detected by a set of multichannel plates (MCPs; Quantar Technology). The MCP signals from the two anodes are amplified and fed into two multichannel scalers (Turbo MCS, EG&G Ortec, Oak Ridge, TN) for counting purposes. Synchronization of the data acquisition with the modulation electronics is achieved by triggering the start pulse of the data acquisition from the sequence generator at the beginning of the first sequence element. The digitized waveform acquired by the multichannel scaler is transferred to a computer (700 MHz Pentium III-based PC, with 384 MB RAM). Real-time deconvolution and data processing is performed with a program written in Delphi.

Mass calibration was achieved by quadratic regression analysis between the flight times and the known molecular weights of caffeine, polypropylene glycol (PPG 450), bradykinin, and reserpine.

Solvents used for preparing the solutions were reagent grade. Bradykinin, caffeine, reserpine (Sigma), and polypropylene glycol standard (PPG 450, narrow molecular-weight distribution; Scientific Polymer Products) were used as received without further purification. The analytes were dissolved in a water:methanol mixture (70:30 v/v). To improve the electrospray ionization efficiency 10 μL of 50 mM sodium acetate solution were added per mL of sample solutions of bradykinin, reserpine, and polypropylene glycol.

Received: July 8, 2004

Keywords: analytical methods · mass spectrometry · time of flight

[1] M. Guilhaus, *J. Mass Spectrom.* **1995**, *30*, 1519–1532; b) M. Guilhaus, V. Mlynski, D. Selby, *Rapid Commun. Mass Spectrom.* **1997**, *11*, 951–962; c) R. J. Cotter, *Anal. Chem.* **1999**, *71*, 445A–451A; d) B. A. Mamyrin, *Int. J. Mass Spectrom.* **2001**, *206*, 251–266.

[2] S. D. Koning, H.-G. Janssen, M. V. Deursen, U. A. T. Brinkman, *J. Sep. Sci.* **2004**, *27*, 397–409; b) M. T. Roberts, J.-P. Dufour, A. C. Lewis, *J. Sep. Sci.* **2004**, *27*, 473–478.

[3] J. B. Fenn, *Angew. Chem.* **2003**, *115*, 3999–4024; *Angew. Chem. Int. Ed.* **2003**, *42*, 3871—3894; b) J. S. Rossier, N. Youhnovski, N. Lion, E. Damoc, S. Becker, F. Reymond, H. H. Girault, M. Przybylski, *Angew. Chem.* **2003**, *115*, 55–60; *Angew. Chem. Int. Ed.* **2003**, *42*, 53–58.

[4] J. A. Olivares, N. T. Nguyen, C. R. Yonker, R. D. Smith, *Anal. Chem.* **1987**, *59*, 1230–1232.

[5] a) F. J. Knorr, M. Ajami, D. A. Chatfield, *Anal. Chem.* **1986**, *58*, 690–694; b) G. Hars, I. Maros, *Int. J. Mass Spectrom.* **1999**, *225*, 101–114.

[6] I. V. Chernushevich, W. Ens, K. G. Standing, *Anal. Chem.* **1999**, *71*, 452A–461A; b) M. Guilhaus, D. Selby, V. Mlynski, *Mass Spectrom. Rev.* **2000**, *19*, 65–107.

[7] a) A. Brock, N. Rodriguez, R. N. Zare, *Anal. Chem.* **1998**, *70*, 3735–3741; b) A. Brock, N. Rodriguez, R. N. Zare, *Rev. Sci. Instrum.* **2000**, *71*, 1306–1318; c) F. M. Fernandez, J. M. Vadillo, F. Engelke, J. R. Kimmel, R. N. Zare, N. Rodriguez, M. Wetterhall, K. Markides, *J. Am. Soc. Mass Spectrom.* **2001**, *12*, 1302–1311; d) F. M. Fernandez, J. M. Vadillo, J. R. Kimmel, M. Wetterhall, K. Markides, N. Rodriguez, R. N. Zare, *Anal. Chem.* **2002**, *74*, 1611–1617; e) J. R. Kimmel, F. M. Fernandez, R. N. Zare, *J. Am. Soc. Mass Spectrom.* **2003**, *14*, 278–286; f) R. N. Zare, F. M. Fernandez, J. R. Kimmel, *Angew. Chem.* **2003**, *115*, 30–36; *Angew. Chem. Int. Ed.* **2003**, *42*, 30–35.

[8] a) N. E. Bradbury, R. A. Nielsen, *Phys. Rev.* **1936**, *49*, 388; b) J. R. Kimmel, F. Engelke, R. N. Zare, *Rev. Sci. Instrum.* **2001**, *72*, 4354–4357.

[9] C. Bolton, *Electronic Design News (EDN)*, October 3, **2002**, 88.

[10] G. E. Yefchak, G. A. Schutz, J. Allison, C. G. Enke, J. F. Holland, *J. Am. Soc. Mass Spectrom.* **1990**, *1*, 440–447.

[11] a) M. Harwit, N. J. A. Sloane, *Hadamard Transform Optics*, Academic Press, New York, **1979**; b) A. G. Marshall, *Fourier, Hadamard, and Hilbert Transforms in Chemistry*, Plenum, New York, **1982**.

[12] M. B. Comisarow, A. G. Marshall, *Chem. Phys. Lett.* **1974**, *25*, 282–283; b) M. B. Comisarow, A. G. Marshall, *Chem. Phys. Lett.* **1974**, *26*, 489–490.

